

H₂O incorporation in the phosphorene/a-SiO₂ interface: A first-principles study

Wanderlã L. Scopel*

*Departamento de Física, Universidade Federal do Espírito Santo, Vitória, ES, 29075-910, Brazil and
Departamento de Ciências Exatas, Universidade Federal Fluminense, Volta Redonda, RJ, 27255-250, Brazil*

Everson S. Souza†

Departamento de Física, Universidade Federal do Espírito Santo, Vitória, ES, 29075-910, Brazil

R. H. Miwa‡

*Departamento de Física, Universidade Federal de Uberlândia,
Caixa Postal 593, CEP 38400-902, Uberlândia, MG, Brazil*

(Dated: August 31, 2016)

Based on first-principles calculations, we investigate the energetic stability and the electronic properties of (i) a single layer phosphorene (SLP) adsorbed on the amorphous SiO₂ surface (SLP/a-SiO₂), and (ii) the further incorporation of water molecules at the phosphorene/a-SiO₂ interface. In (i), we find that the phosphorene sheet bonds to a-SiO₂ through van der Waals interactions, even upon the presence of oxygen vacancy on the surface. The SLP/a-SiO₂ system presents a type-I band alignment, with the valence (conduction) band maximum (minimum) of the phosphorene lying within the energy gap of the a-SiO₂ substrate. The structural, and the surface-potential corrugations promote the formation of electron-rich and -poor regions on the phosphorene sheet and at the SLP/a-SiO₂ interface. Such charge density puddles have been strengthened by the presence of oxygen vacancies in a-SiO₂. In (ii), due to the amorphous structure of the surface, we have considered a number of plausible geometries of H₂O embedded in the SLP/a-SiO₂ interface. There is an energetic preference to the formation of hydroxyl (OH) groups on the a-SiO₂ surface. Meanwhile, upon the presence of oxygenated water or interstitial oxygen in the phosphorene sheet, we find the formation of metastable OH bonded to the phosphorene, and the formation of energetically stable P–O–Si chemical bonds at the SLP/a-SiO₂ interface. Further x-ray absorption spectra (XAS) simulations have been done, aiming to provide additional structural/electronic informations of the oxygen atoms forming hydroxyl groups or P–O–Si chemical bonds at the interface region.

I. INTRODUCTION

Phosphorene is a two-dimensional (2D) material, consisting of a single-layer of the black phosphorus allotrope that, currently, has received tremendous attention. It presents unique properties, such as layer-controlled direct bandgap [1, 2], high-mobility [3], and *p*-type semiconductor properties [4]. These properties make phosphorene a quite interesting 2D material for electronic applications [5–9].

There are two main methods to produce phosphorene, both based on the exfoliation processes down to a monolayer thickness, *viz.*: mechanical exfoliation [10–12] and liquid exfoliation [13–15]. However, exfoliated phosphorus degrades when exposed in ambient conditions [16, 17]. Such a phosphorene degradation [11, 18] is an irreversible process, ascribed to the presence of oxygen atoms, and water molecules. Indeed, phosphorene presents lower chemical stability due to the lone pairs of the surface P atoms, which leads it to be very reactive when exposed to air. In Ref. [19] the authors have been shown that oxy-

gen interstitial defect on phosphorene lead to increasing of hydrophilicity of the surface, which may play an important role in the surface degradation. Further studies have been done in an effort to understand the degradation of phosphorene upon the presence of O₂ and/or H₂O molecules [11, 20–22], as well as some proposals to avoid it. For instance, phosphorene surface passivation through Al₂O₃ coating [23–25].

The degradation process of phosphorene is strongly correlated with its boundary conditions. In a recent experimental study, Wood *et al.* [22] verified that the degradation of transistors, composed by few layers of phosphorene, can be suppressed upon the presence of a hydrophilic substrate (SiO₂) and a coating layer of AlO_x. Since SiO₂ surface is by far the most common substrate to buildup transistors, it is quite important to get a clear picture of the electronic interactions and the structural properties of (i) phosphorene adsorbed on the SiO₂ surface, as well as (ii) the role played the SiO₂ surface in the phosphorene degradation mediated by the presence of H₂O molecules.

In this work, we performed an atomistic study, based on first-principles calculations of (i) and (ii) described above. We have considered a single layer phosphorene (SLP) adsorbed on the amorphous SiO₂ surface (SLP/a-SiO₂). In (i), we found that the SLP bonds to the a-

* wlscope@if.uff.br

† nosreveazuos@gmail.com

‡ hiroki@infis.ufu.br

SiO₂ surface mediated by van der Waals (vdW) interactions, even upon the presence of oxygen vacancies (V_O), which is the most common intrinsic defect in SiO₂. The structural, and the surface-potential corrugations promote the formation of electron-rich and -poor regions on the phosphorene sheet, and at the phosphorene/a-SiO₂ interface. Such charge density puddles are strengthened by the presence of oxygen vacancies in a-SiO₂. In (ii), we have considered a number of plausible configurations for the H₂O molecules embedded in the SLP/a-SiO₂ interface. We find an energetic preference for the formation of hydroxyl (OH) groups bonded to the a-SiO₂ surface, when compared with the SLP, even upon the presence of the interstitial oxygen adatoms in the SLP sheet. However, due to the amorphous character of the a-SiO₂ surface, depending on the local geometry at the SLP/a-SiO₂ interface region, we verified the formation of energetically stable P–O–Si structure bridging the SLP sheet and the a-SiO₂ surface. Finally, x-ray absorption spectra (XAS) simulations have been done, aiming to provide additional structural/electronic informations of the oxygen atoms forming hydroxyl groups or P–O–Si chemical bonds at the interface region.

II. METHODOLOGY

The amorphous structure was generated through *ab initio* molecular dynamics (MD) simulations based on the density functional theory (DFT) approach, as implemented in the VASP code [26–28]. In Ref. [29], we present details on the generation procedure of amorphous SiO₂ bulk structure. For DFT calculations, the generalized gradient approximation (GGA) for the exchange-correlation potential is used. The ion-electron interaction is treated with the projected augmented wave (PAW) [30, 31] method. The plane-wave cutoff energy for wave function is set to 500 eV and the Brillouin zone was sampled at the Γ point. All atoms were allowed to relax until the atomic forces were smaller than 0.025 eV/Å. In addition, a combination of optB88vdW [32, 33] for geometry optimization and HSE06 [34] for density of state (based on the optB88-vdW optimized structure) is used, which has been shown very reliable for single-layer phosphorene (SLP). The slab model contains three different atomic species with vacuum region of ca. 15 Å, so that the interaction between successive periodic images along to z-direction can be neglected. The optimized lattice parameter for single-layer phosphorene (SLP) was $a = 4.38$ Å and $b = 3.31$ Å, in good agreement with previous theoretical and experimental results [4, 35]. In our calculations we used a 3×4 supercell size.

III. RESULTS AND DISCUSSIONS

A. SLP/a-SiO₂ interface

Initially we examine the energetic stability of a SLP adsorbed on the defect-free amorphous SiO₂ surface (SLP/a-SiO₂). In Fig. 1(a1) we present the structural model and the electronic charge transfers (which will be discussed below) of SLP/a-SiO₂. The energetic stability of the SLP adsorbed on the SiO₂ surface was examined by the calculation of the adsorption energy (E^a), which can be written as,

$$E^a = E[\text{a-SiO}_2] + E[\text{SLP}] - E[\text{SLP/a-SiO}_2].$$

Where $E[\text{SLP}]$ and $E[\text{a-SiO}_2]$ are the total energies of the separated components, an isolated SLP, and the a-SiO₂ surface, respectively; $E[\text{SLP/a-SiO}_2]$ is the total energy of the fully relaxed SLP/a-SiO₂ system. It was considered the adsorption of SLP on two different (amorphous) SiO₂ surfaces, where we found adsorption energies of 13.9 and 11.3 eV/Å², and (averaged) vertical distances between the SLP and the a-SiO₂ surface of 2.80 and 2.75 Å. Thus, suggesting the absence of chemical bonds at the SLP–surface region. The SLP sheet is attached to the a-SiO₂ surface mediated by vdW interactions. Somewhat similar picture has been verified for other 2D systems adsorbed on a-SiO₂. For instance, we obtained E^a of 6.3 and 15 meV/Å² for graphene and MoS₂ on the a-SiO₂ surface, [36, 37].

Due to the surface corrugation, SLP on a-SiO₂ may also present structural deformations, as observed for graphene on a-SiO₂ [38, 39]; giving rise to electron-rich and -poor regions (so called electron-hole puddles) on the graphene surface [40]. Indeed, due to corrugation of the (amorphous) surface potential, and the vertical distortion of ~ 0.08 Å of the SLP adsorbed on a-SiO₂, we also verify the formation of electron-hole puddles on the SLP surface, as well as electronic charge transfers at the SLP–a-SiO₂ interface region. Here, we map the total charge transfers ($\Delta\rho$) by comparing total charge density of the final system, SLP/a-SiO₂ ($\rho[\text{SLP/a-SiO}_2]$) with the ones of the isolated components, SLP ($\rho[\text{SLP}]$) and a-SiO₂ ($\rho[\text{a-SiO}_2]$),

$$\Delta\rho = \rho[\text{SLP/a-SiO}_2] - \rho[\text{SLP}] - \rho[\text{a-SiO}_2].$$

Our result of $\Delta\rho$ for a SLP on the pristine a-SiO₂ surface is presented in Fig. 1(a1). In Fig. 1(a2) we present the planar average of $\Delta\rho$ perpendicularly to the surface plane, $\Delta\rho(z)$. The electronic charge transfer is (i) not uniform on the surface plane, and (ii) mostly localized at the interface region, where we have both positive as negative values of $\Delta\rho$. In order to quantify the total charge transfers, we have used the Bader charge density analysis [41, 42]; where we found that the total charge density of the SLP reduces by $6.70 \times 10^{12} e/\text{cm}^2$.

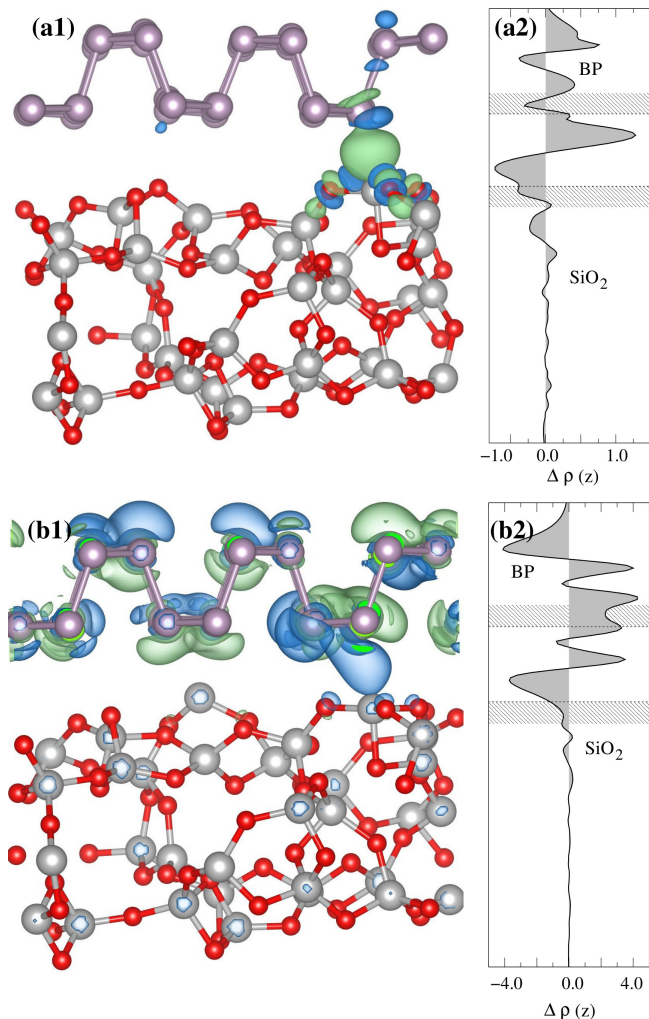


FIG. 1. (a1) Structural model and the electronic charge transfers ($\Delta\rho$) of a single layer phosphorene adsorbed on the a-SiO₂ surface (SLP/a-SiO₂); (a2) planar average of the net charge transfer perpendicularly to the SLP/a-SiO₂ interface. (b1) Structural model and the electronic charge transfers of SLP/a-SiO₂ upon the presence of an intrinsic defect on the surface, oxygen vacancy; (b2) planar average of the net charge transfer perpendicularly to the SLP/a-SiO₂ interface. Green regions indicate an increase of total charge density, $\Delta\rho > 0$, while blue regions indicate a decrease ($\Delta\rho < 0$). The P, O, Si and H atoms are represented by light purple, red and gray color spheres.

The SLP–SiO₂ interaction has been strengthened upon the presence of oxygen vacancies. We found that the adsorption energy increases to 16.6 meV/Å², and there is a net charge transfer of $1.06 \times 10^{13} e/\text{cm}^2$ ($0.19 e/V_O$ defect), from the surface to the SLP. In Figs. 1(b1) and 1(b2), we present our results of $\Delta\rho$ and $\Delta\rho(z)$, respectively. It noticeable that the most of the charge density gain is localized on the lower zigzag chains of the phosphorene; somewhat similar picture has been verified for the the n-type doped graphene bilayers on

the Cu(111) surface [43]. It is worth noting the formation electron-rich ($\Delta\rho > 0$, green regions) and electron-poor ($\Delta\rho < 0$, blue regions) embedded in the phosphorene layer, Fig. 1(b1), while $\Delta\rho \approx 0$ in the SiO₂ surface. As verified for graphene on SiO₂ [36, 40], those electron-rich and -poor regions, randomly distributed on the phosphorene layer, are ruled by the structural deformation of the adsorbed SLP, and the corrugation of the a-SiO₂ surface potential.

Focusing on the electronic properties, we calculate the energy positions of the valence band maximum (VBM), and conduction band minimum (CBM) of the isolated components, and the ones of the final system, SLP/a-SiO₂, Fig. 2. The energy positions were aligned with respect to the vacuum level [44]. For the SLP we find an ionization potential of 5.3 eV, and an energy gap of 1.55 eV, which are in good agreement with recent theoretical studies [2, 45, 46]. Meanwhile, for the a-SiO₂ we find an energy gap of 6.15 eV, and an ionization potential of 8.4 eV. In Fig. 2(a2) we present the density of states (DOS) (shaded region) and the projected density of states (PDOS) on the SLP (dashed lines) and SiO₂ (solid lines). The VBM and the CBM of the SLP are slightly perturbed (by about 0.1 meV) upon its interaction with the a-SiO₂ surface, being both localized within the energy gap of the a-SiO₂. In this case, the SLP–a-SiO₂ interface presents a type-I band alignment, with valence band offset (VBO) and conduction band offset (CBO) of about 3.11 and 1.47 eV, respectively. Here we are not considering the contribution of the dipole effects, at the SLP–a-SiO₂ interface region, on the band VBM and CBM band alignment [47].

A single oxygen vacancy on the a-SiO₂ surface gives rise to an occupied defect level within the energy gap of a-SiO₂. Here, we find the an occupied defect level lying at VBM+1.60 eV [Fig. 2(b1)], in good agreement with previous theoretical work [48]. Upon the formation of SLP/a-SiO₂, the defect level is resonant with the VBM of the adsorbed SLP sheet, Figs. 2(b1) and 2(b2); meanwhile the energy positions of the VBM and CBM of SLP are weakly perturbed by the presence of the V_O defect.

B. H₂O at SLP/SiO₂ interface

Here, initially we examine the energetic stability of water molecules adsorbed on the separated components, *viz.*: water on SLP (H₂O/SLP), and on the amorphous a-SiO₂ surface (H₂O/a-SiO₂). For the former system, we have considered two (energetically stable) H₂O/SLP configurations, Figs. 3(a) and 3(b); both recently proposed in the literature [20, 21]. We found that those two structures are very close in energy, where we obtained H₂O adsorption energies of 0.18 and 0.21 eV/molecule, respectively. Our total energy results support the “two leg” geometry recently proposed by Wang *et al.* [21]. At the equilibrium geometry, the molecular structure of H₂O has been preserved, lying at 2.50 Å from the SLP surface.

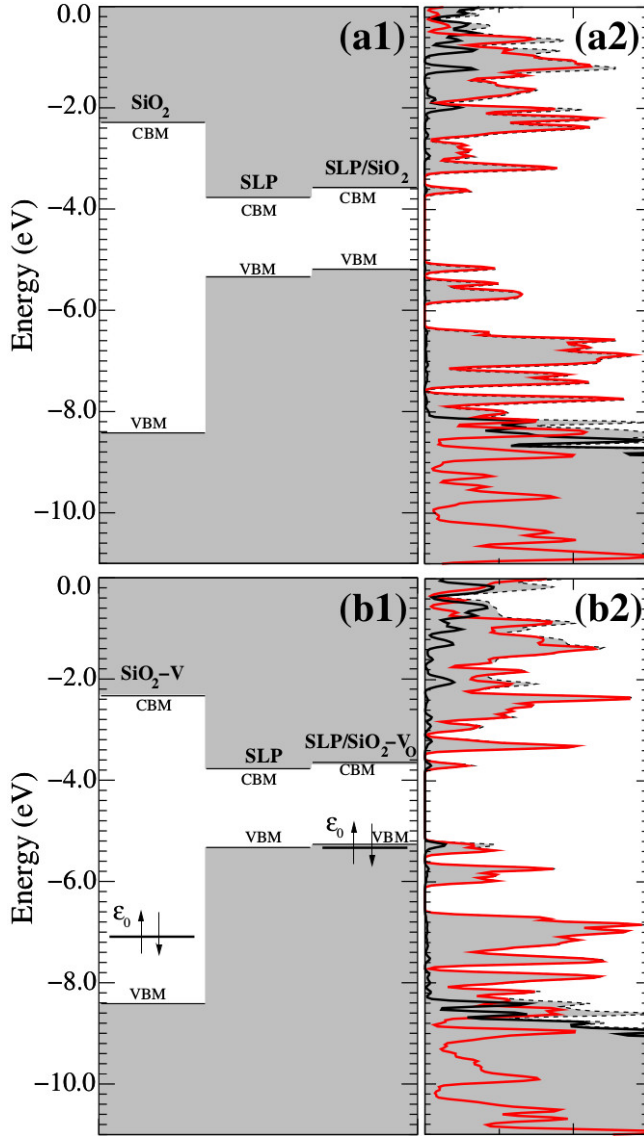


FIG. 2. Electronic energy levels of the valence band maximum (VBM) and the conduction band minimum (CBM) of the isolated components, SLP and a-SiO₂, and the ones of the final system, SLP/a-SiO₂, and the projected density of states (PDOS), of the pristine surface (a1-a2), and upon the presence of an oxygen vacancy (b1-b2). ϵ_0 indicate the energy position of the (oxygen vacancy) defect level.

There are several studies addressing the adsorption of water molecules on silica surfaces. The subject becomes more complicated and interesting for amorphous surfaces, since we have a very large number of energetically metastable configurations of H₂O on a-SiO₂. Here we have considered two different geometries, *viz.*: (i) a H₂O molecule attached to the four-fold coordinated surface Si atom [H₂O/a-SiO₂ in Fig. 3(c)], and (ii) H₂O dissociated geometry, giving rise to two hydroxyls, one composed by the oxygen and hydrogen atoms remnant from the adsorbed H₂O molecule, and another composed by

a H atom, dissociated from the original H₂O molecule, bonded to the two-fold coordinate oxygen atom of the a-SiO₂ surface [OH/(OH)a-SiO₂ in Fig. 3(d)]. In (i) we find an adsorption energy of 1.19 eV/molecule, with Si-O equilibrium bond length of 1.82 Å (close to the sum of the covalent radii of Si and O, 1.83 Å), indicating the formation of chemical bond between the H₂O molecule and the a-SiO₂ surface. Our adsorption energy, and Si-O bond length results are in good agreement with the ones obtained by Zhao and Jing [49], for H₂O adsorbed on SiO₂ clusters. On the other hand, we find that once the H₂O molecule is adsorbed on the a-SiO₂ surface, the formation of hydroxyl groups [(ii)], H₂O/a-SiO₂ → OH/(OH)a-SiO₂, is an exothermic process by 1.45 eV. Indeed, the formation of OH groups on a-SiO₂ has been supported by other theoretical studies [50–52], and it is in agreement with the experimental observation [53]. Those adsorption energy results allow us to confirm the hydrophilic character of the a-SiO₂ surface with respect to the SLP. In a recent experimental study, performed by Wood *et al.* [22], the authors verified that the oxidation rate, of exfoliated black phosphorous, has been reduced by the presence of the (hydrophilic) SiO₂ surface.

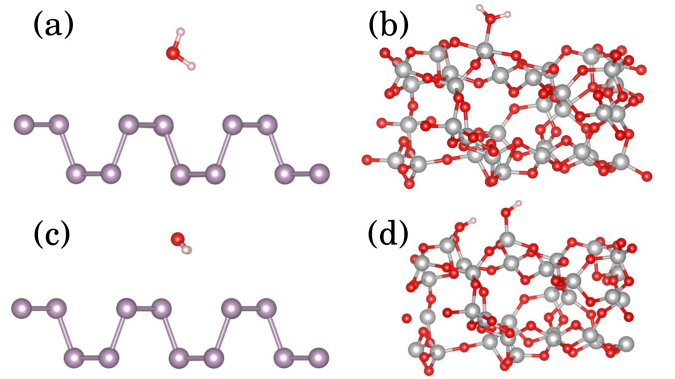


FIG. 3. Equilibrium geometries of the H₂O molecule adsorbed on the single layer phosphorene (a) and (c); and on the a-SiO₂ surface (b) and (d). The P, O, Si and H atoms are represented by light purple, red, gray and white color spheres.

Next we examine the presence of H₂O at the SLP–a-SiO₂ interface region. Within our calculation approach, the interactions between the H₂O molecules are negligible; we are considering lateral distances of about 13 Å between the molecules, which corresponds to a planar concentration of $5.6 \times 10^{13}/\text{cm}^2$. At such a low coverage regime, the adsorption energy of SLP on the H₂O/a-SiO₂ surface [SLP/H₂O/a-SiO₂ in Fig. 4(a)] is practically the same as that obtained without H₂O molecules. We have considered two SLP/H₂O/a-SiO₂ configurations, where we found E^a of 13.2 and 15.8 meV/Å², and the vertical distance between the SLP and the a-SiO₂ surface increases to 3.47 Å (averaged value).

Similarly to the H₂O/a-SiO₂ systems discussed above, the formation of hydroxyl groups even at the presence

of the SLP layer, $\text{SLP}/\text{H}_2\text{O}/\text{a-SiO}_2 \rightarrow \text{SLP}/\text{OH}/(\text{OH})\text{a-SiO}_2$ [Fig. 4(b)], is an exothermic process; the total energy reduces by 1.23 eV. The presence of hydroxyl groups at the SLP–a-SiO₂ interface increases the corrugation of the SLP by 0.14 Å, in comparison with the SLP/a-SiO₂ system, 0.08→0.22 Å, where the SLP lies at 2.50 Å from the (OH)/(OH)a-SiO₂ substrate (averaged values). Indeed, similar equilibrium geometry picture has been verified for graphene adsorbed on a-HfO₂, intercalated by H₂O molecules [54].

In order to provide a more complete picture of water in SLP/a-SiO₂, we have also considered the presence of oxygen, (i) as a interstitial defect attached to the SLP, and (ii) forming oxygenated H₂O, embedded between the phosphorene sheet and the a-SiO₂ substrate [22]. For the interstitial oxygen, our binding energy, and equilibrium geometry results are in agreement with the ones of the most stable configuration predicted by Ziletti *et al.* [19].

The structural model, and the total energy differences in (i) are depicted in Figs. 4(c)–4(e); by comparing the total energies, we found the latter (former) configuration as the most (less) stable one. Thus, indicating that, even at the presence of interstitial oxygen attached to the SLP, the remnant H atom from the H₂O molecule promotes the formation hydroxyls on the a-SiO₂ surface, Fig. 4(e), as we verified on the a-SiO₂ pristine surface. In this case, there is an atomic rearrangement on the a-SiO₂ surface, in order to keep the two-fold (four-fold) coordination of the surface O (Si) atoms. However, it is worth noting that due to the amorphous character of the surface, the formation of hydroxyl groups on a-SiO₂ will depend on the local geometry, and thus, although energetically less stable, we may find the formation of hydroxyl groups on the SLP, as shown in Fig. 4(d).

In (ii), we find that dissociation of H₂O₂, giving rise to hydroxyl groups attached to the SLP or a-SiO₂ surface, is an exothermic process. Here we have considered a number of plausible configurations of OH at the SLP–a-SiO₂ interface. For an OH group attached to the SLP sheet, Fig. 4(f), we find a total energy release of 0.99 eV/OH, when compared with the separated components, namely, pristine SLP/a-SiO₂ and a H₂O₂ molecule. Further total energy comparisons indicate that the SLP/(OH)a-SiO₂ configuration [Fig. 4(g)] is more stable by 1.13 eV. Whereas, again due to the amorphous character of the surface, we may find an energetically quite stable configuration composed by an oxygen atom (two fold coordinated) forming a P–O–Si bridge structure between the SLP and the a-SiO₂ surface; while the remnant hydrogen atom forms an OH group with the a-SiO₂ surface, Fig. 4(h).

X-ray absorption spectroscopy (XAS) has been considered a quite suitable technique to provide informations about atomic and electronic structure near the probed element. Here, we characterize the presence of OH groups by performing a set of XAS simulations of the oxygen K-edge spectrum in SLP/a-SiO₂.

Initially, in order to verify the adequacy of our calcu-

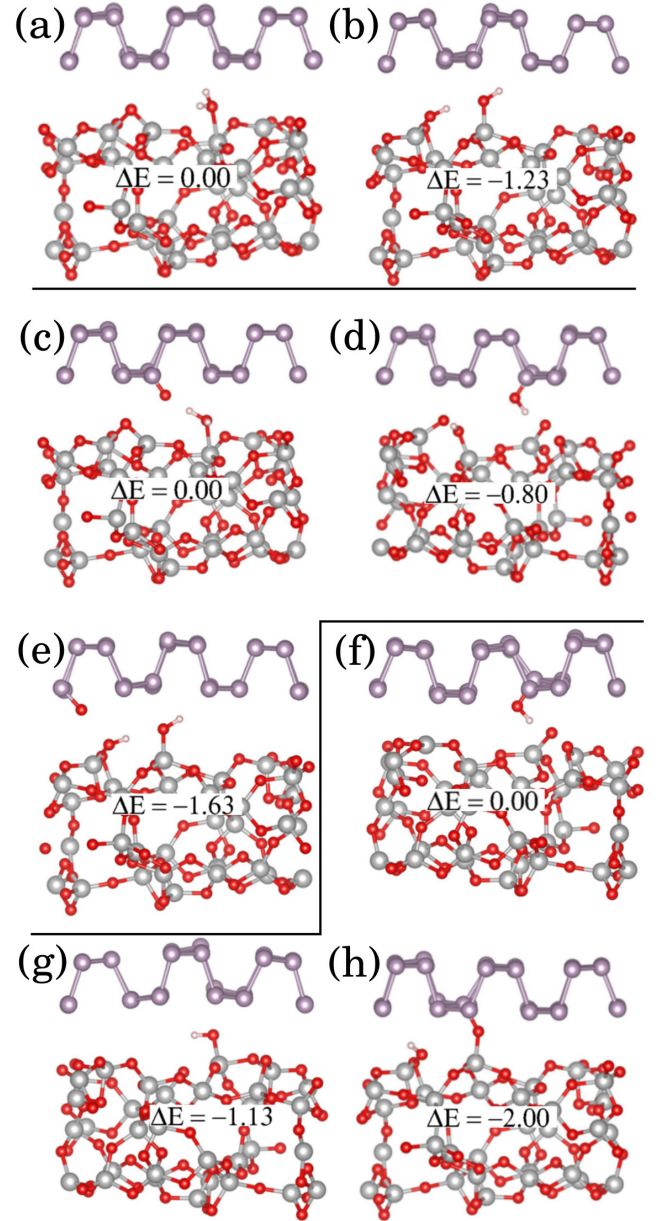


FIG. 4. Equilibrium geometries of H₂O molecules embedded in the SLP/a-SiO₂ interface, undissociated (a), and dissociated forming OH groups (b). Equilibrium geometries of H₂O molecules intercalated between the oxidized SLP and the a-SiO₂ surface, undissociated (c), dissociate forming an OH group bonded to the SLP and another bonded to the a-SiO₂ surface (d), and forming two OH groups bonded to the a-SiO₂ surface (e). Equilibrium geometry of an OH group bonded to the SLP (f), an OH group bonded to the a-SiO₂ (g), and an oxygen atoms forming a P–O–Si bridge structure (h). The P, O, Si and H atoms are represented by light purple, red and gray color spheres.

lation procedure, we calculated the oxygen K-edge spectrum of α -quartz (SiO₂). Where, as shown in Fig. 5 (solid lines), we find a good agreement with the previous the-

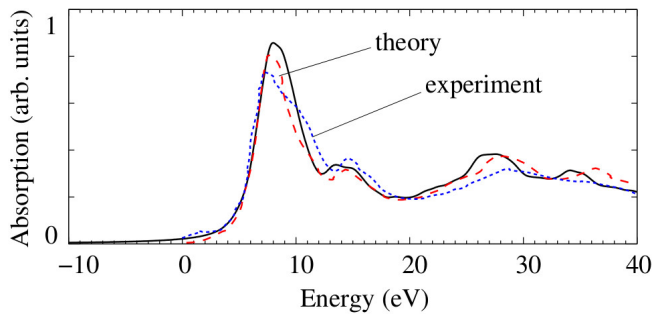


FIG. 5. Oxygen K-edge XANES spectrum obtained for the α -quartz geometry comparing with experimental and theoretical data[55].

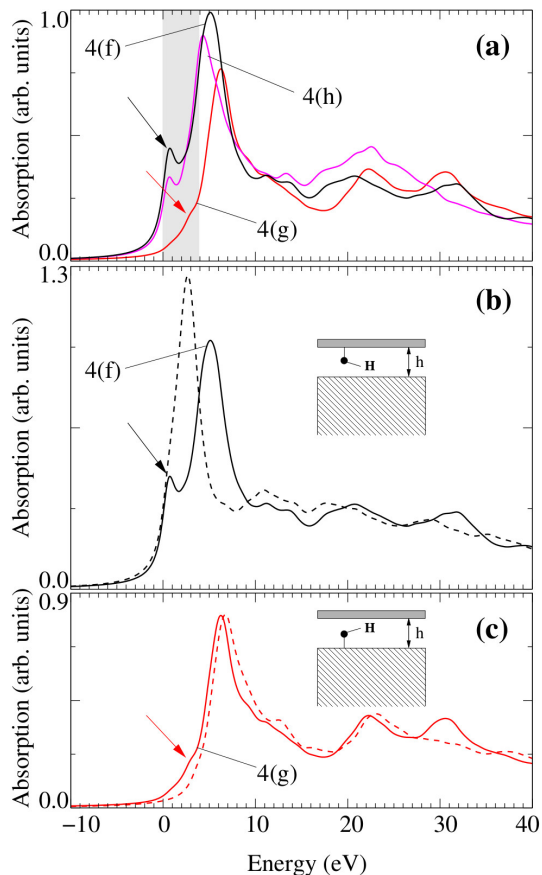


FIG. 6. Simulated oxygen K-edge XAS spectrum of the OH group for structural models depicted in Figs. 4(f), 4(g), and 4(h) (a). O K-edge spectrum of the OH group of the structural models shown in Fig. 4(f) and 4(g). (b) at the equilibrium geometry ($h=2.00$ Å, solid-line) and increasing the vertical distance ($h=4.00$ Å, dashed-line), and (c) at the equilibrium geometry ($h=2.82$ Å, solid-line) and increasing the vertical distance ($h=6.82$ Å, dashed-line).

oretical/experimental findings [55]. For the SLP/a-SiO₂, we examine the K-edge spectrum of the oxygen atom of the OH group, as shown in Figs. 4(f) and 4(g), as well as

the one forming the P-O-Si bridge structure presented in Fig. 4(h). Based on the PDOS results, shown in Fig. 2(a), the final state in the O-1s \rightarrow p transition should present a dominant contribution from the P-3p orbitals of the SLP; even upon the presence of a core hole in the (probed) oxygen atom. Thus, suggesting a weak dependence between the O K-edge energy position and the configuration of the oxygen atom in SLP/a-SiO₂. Indeed, for the three structural models, the XAS spectra present somewhat the same feature, with the O-1s peak lying within the shaded region in Fig. 6(a). Indicated by arrows in Fig. 6(a), we verify that the O-1s peak is more intense for OH group bonded to the SLP [structural model shown in Fig. 4(f)], and less intense for OH bonded to the SiO₂ surface [Fig. 4(g)]. Meanwhile, for O atom forming the P-O-Si bridge structure, Fig. 4(h), we have an intermediate intensity.

Computational simulations can be a quite useful tool to help the interpretation of XAS spectra. For instance, we can simulate a set of configurations, which are experimentally non-accessible, aiming to provide additional informations of a given spectrum. In Fig. 6(b), the solid line indicate the original O K-edge spectrum of OH bonded to the SLP [Fig. 4(f)]; while the dashed line corresponds to the O K-edge spectrum of the same OH configuration, but increasing the vertical distance (h) from 2.00 Å (equilibrium geometry) to 4.00 Å. In this case, the role played by the a-SiO₂ surface, to the XAS spectrum, has been reduced. We find that the two (original) O-1s peaks reduce to a single one with higher intensity. Thus, indicating that (i) the a-SiO₂ surface orbitals contribute to the final state of O K-edge spectrum of OH bonded to the SLP, and (ii) the interaction with the a-SiO₂ surface reduces the O-1s binding energy. On the other hand, for OH group bonded to the a-SiO₂ surface [Fig. 4(g)], (i) the feature indicated by an arrow in Fig. 6(c) has been suppressed by increasing the vertical distance, $h = 2.82$ (equilibrium position) \rightarrow 6.82 Å, and (ii) there is an increase on the O-1s binding energy. Those results can be attributed to the reduction of electronic contributions from the phosphorene to the final state of O K-edge spectrum.

IV. SUMMARY

In summary, based on first-principles calculations we investigate (i) the electronic and structural properties of a single layer phosphorene (SLP) adsorbed on the amorphous silicon oxide surface (SLP/a-SiO₂), and (ii) the incorporation of H₂O molecules in the SLP-a-SiO₂ interface. In (i), we find that single layer phosphorene bonds to the amorphous SiO₂ surface (SLP/a-SiO₂) mediated by vdW interactions. There are no chemical bonds between the SLP and the surface, even at the presence of oxygen vacancies (V_O), which is a common intrinsic defect in a-SiO₂. The (amorphous) surface corrugation promotes a non-uniform charge density distribution, giv-

ing rise to electron-hole puddles in SLP/a-SiO₂. Such charge density puddles are strengthened upon the presence of V_O, which may reduce the carrier mobility in the phosphorene layer. The V_O defect gives rise to an occupied level in the band gap of a-SiO₂; upon the formation of SLP/a-SiO₂, the defect level lies near the valence band maximum of the SLP. We estimate the band alignment of SLP/a-SiO₂, where we find a type-I band offset. In (ii), we find an energetic preference for the formation of hydroxyl (OH) groups bonded to the pristine a-SiO₂ surface, as well as upon the presence of the SLP, SLP/a-SiO₂. However, due to the amorphous structure of the surface, depending on the local geometry, we may find other energetically stable configurations. Indeed, we found one composed by an hydrogen atom bonded to the

a-SiO₂ surface and the oxygen atom forming a P–O–Si bridge structure. Further x-ray absorption spectroscopy (XAS) simulations, of oxygen atom forming OH or P–O–Si bridge structure, reveal that the K-edge spectra present different features for each configuration.

ACKNOWLEDGMENTS

The authors acknowledge the support from Brazilian agencies CNPq, FAPES, FAPEMIG and CAPES; we thank also to CENAPAD-SP for computer time.

REFERENCES

- [1] S. Zhang, J. Yang, R. Xu, F. Wang, W. Li, M. Ghufuran, Y.-W. Zhang, Z. Yu, G. Zhang, Q. Qin, *et al.*, ACS nano **8**, 9590 (2014).
- [2] V. Tran, R. Soklaski, Y. Liang, and L. Yang, Physical Review B **89**, 235319 (2014).
- [3] J. Qiao, X. Kong, Z.-X. Hu, F. Yang, and W. Ji, Nature communications **5** (2014).
- [4] H. Liu, A. T. Neal, Z. Zhu, Z. Luo, X. Xu, D. Tománek, and P. D. Ye, ACS nano **8**, 4033 (2014).
- [5] L. Li, Y. Yu, G. J. Ye, Q. Ge, X. Ou, H. Wu, D. Feng, X. H. Chen, and Y. Zhang, Nature nanotechnology **9**, 372 (2014).
- [6] S. Das, M. Demarteau, and A. Roelofs, ACS nano **8**, 11730 (2014).
- [7] W. Zhu, M. N. Yogeesh, S. Yang, S. H. Aldave, J.-S. Kim, S. Sonde, L. Tao, N. Lu, and D. Akinwande, Nano letters **15**, 1883 (2015).
- [8] Y. Du, H. Liu, Y. Deng, and P. D. Ye, ACS nano **8**, 10035 (2014).
- [9] H. Du, X. Lin, Z. Xu, and D. Chu, Journal of Materials Chemistry C **3**, 8760 (2015).
- [10] I. Verzhbitskiy, A. Carvalho, A. S. Rodin, S. P. Koenig, G. Eda, W. Chen, A. C. Neto, and B. Ozyilmaz, ACS nano **9**, 8070 (2015).
- [11] A. Favron, E. Gaufrès, F. Fossard, A.-L. Phaneuf-LHeureux, N. Y. Tang, P. L. Lévesque, A. Loiseau, R. Leonelli, S. Francoeur, and R. Martel, Nature Materials **14**, 826 (2015).
- [12] W. Lu, H. Nan, J. Hong, Y. Chen, C. Zhu, Z. Liang, X. Ma, Z. Ni, C. Jin, and Z. Zhang, Nano Research **7**, 853 (2014).
- [13] Z. Guo, H. Zhang, S. Lu, Z. Wang, S. Tang, J. Shao, Z. Sun, H. Xie, H. Wang, X.-F. Yu, *et al.*, Advanced Functional Materials **25**, 6996 (2015).
- [14] J. R. Brent, N. Savjani, E. A. Lewis, S. J. Haigh, D. J. Lewis, and P. O'Brien, Chemical Communications **50**, 13338 (2014).
- [15] J. Kang, J. D. Wood, S. A. Wells, J.-H. Lee, X. Liu, K.-S. Chen, and M. C. Hersam, ACS nano **9**, 3596 (2015).
- [16] S. P. Koenig, R. A. Doganov, H. Schmidt, A. C. Neto, and B. Ozyilmaz, Applied Physics Letters **104**, 103106 (2014).
- [17] A. H. Woomer, T. W. Farnsworth, J. Hu, R. A. Wells, C. L. Donley, and S. C. Warren, ACS nano **9**, 8869 (2015).
- [18] J. O. Island, G. A. Steele, H. S. van der Zant, and A. Castellanos-Gomez, 2D Materials **2**, 011002 (2015).
- [19] A. Ziletti, A. Carvalho, D. K. Campbell, D. F. Coker, and A. C. Neto, Physical Review Letters **114**, 046801 (2015).
- [20] Y. Cai, Q. Ke, G. Zhang, and Y.-W. Zhang, The Journal of Physical Chemistry C **119**, 3102 (2015).
- [21] G. Wang, W. J. Slough, R. Pandey, and S. P. Karna, 2D Materials **3**, 025011 (2016).
- [22] J. D. Wood, S. A. Wells, D. Jariwala, K.-S. Chen, E. Cho, V. K. Sangwan, X. Liu, L. J. Lauhon, T. J. Marks, and M. C. Hersam, Nano letters **14**, 6964 (2014).
- [23] J. Na, Y. T. Lee, J. A. Lim, D. K. Hwang, G.-T. Kim, W. K. Choi, and Y.-W. Song, ACS nano **8**, 11753 (2014).
- [24] J.-S. Kim, Y. Liu, W. Zhu, S. Kim, D. Wu, L. Tao, A. Dodabalapur, K. Lai, and D. Akinwande, Scientific Reports **5**, 8989 (2015).
- [25] J. Pei, X. Gai, J. Yang, X. Wang, Z. Yu, D.-Y. Choi, B. Luther-Davies, and Y. Lu, Nature communications **7** (2016).
- [26] G. Kresse and J. Hafner, Phys. Rev. B **47**, 558 (1993).
- [27] G. Kresse and J. Hafner, Phys. Rev. B **48**, 13115 (1993).
- [28] G. Kresse and J. Furthmüller, Comput. Mater. Sci. **6**, 15 (1996).
- [29] W. L. Scopel, A. J. R. da Silva, and A. Fazzio, Phys. Rev. B **77**, 172101 (2008).
- [30] P. E. Blöchl, Phys Rev B **50**, 17953 (1994).
- [31] G. Kresse and D. Joubert, Physical Review B **59**, 1758 (1999).
- [32] M. Dion, H. Rydberg, E. Schröder, D. C. Langreth, and B. I. Lundqvist, Physical review letters **92**, 246401 (2004).
- [33] J. Klimeš, D. R. Bowler, and A. Michaelides, Physical Review B **83**, 195131 (2011).
- [34] G. E. S. J. Heyd and M. Ernzerhof, J. Chem. Phys. **124**, 219906 (2006).
- [35] A. Brown and S. Rundqvist, Acta Crystallographica **19**, 684 (1965).

- [36] R. H. Miwa, T. M. Schmidt, W. L. Scopel, and A. Fazzio, *Appl. Phys. Lett.* **99**, 163108 (2011).
- [37] W. Scopel, R. Miwa, T. Schmidt, and P. Venezuela, *Journal of Applied Physics* **117**, 194303 (2015).
- [38] M. Ishigami, J. H. Chen, W. G. Cullen, M. S. Fuhrer, and E. D. Williams, *Nano Lett.* **7**, 1643 (2007).
- [39] A. Sinitskii, D. V. Kosynkin, A. Dimiev, and T. J. M, *ACS Nano* **4**, 3095 (2010).
- [40] J. Martin, N. Akerman, G. Ulbricht, T. Lohmann, J. H. Smet, and K. Von Klitzing, *Nat. Phys.* **4**, 144 (2008).
- [41] R. F. W. Bader, *Atoms in Molecules: A Quantum Theory* (Oxford University Press, New York, 1990).
- [42] W. Tang, E. Sanville, and G. Henkelman, *J. Phys. : Condens. Matter* **21**, 084204 (2009).
- [43] E. S. Souza, W. L. Scopel, and R. Miwa, *Physical Review B* **93**, 235308 (2016).
- [44] Here, the vacuum level was obtained by computing the planar-averaged electrostatic potential perpendicularly to the surface plane.
- [45] Y. Cai, G. Zhang, and Y.-W. Zhang, *Scientific reports* **4** (2014).
- [46] P. Srivastava, K. P. Hembram, H. Mizuseki, K.-R. Lee, S. S. Han, and S. Kim, *The Journal of Physical Chemistry C* **119**, 6530 (2015).
- [47] Since there are no chemical bonding at the SLP-a-SiO₂ interface region, the dipole effect on the band alignment should be small.
- [48] P. Sushko, S. Mukhopadhyay, A. Stoneham, and A. Shluger, *Microelectronic engineering* **80**, 292 (2005).
- [49] L.-l. Zhi, G.-f. Zhao, L.-j. Guo, and Q. Jing, *Physical Review B* **77**, 235435 (2008).
- [50] T. R. Walsh, M. Wilson, and A. P. Sutton, *Journal of Chemical Physics* **113**, 9191 (2000).
- [51] T. Mahadevan and S. Garofalini, *The Journal of Physical Chemistry C* **112**, 1507 (2008).
- [52] G. K. Lockwood and S. H. Garofalini, *The Journal of Physical Chemistry C* **118**, 29750 (2014).
- [53] Y. Kim, T. Wei, J. Stultz, and D. Goodman, *Langmuir* **19**, 1140 (2003).
- [54] E. J. Olson, R. Ma, T. Sun, M. A. Ebrish, N. Haratipour, K. Min, N. R. Aluru, and S. J. Koester, *ACS applied materials & interfaces* **7**, 25804 (2015).
- [55] M. Taillefumier, D. Cabaret, A.-M. Flank, and F. Mauri, *Physical Review B* **66**, 195107 (2002).